Implementation aspects of Field Oriented Control of an Induction Machine for a Hybrid Electric Vehicle

Kristof Engelen[1], Sven De Breucker[1, 2] and Johan Driesen[1]

[1]Esat-Electa, KULeuven, Kasteelpark Arenberg 10, Heverlee, 3001, Belgium
[2] ETE, VITO, Boeretang 200, Mol, 2400, Belgium
E-mail: kristof.engelen1@esat.kuleuven.be, sven.debreucker@ vito.be

Abstract—The aim of this paper is to describe the practical aspects involved with the implementation of field oriented control (FOC) applied to a model hybrid electric vehicle (HEV) [1]. The well-established theory of FOC is described and translated into different implementation steps. In this paper we aspire to fill the gap between theory and practice. The paper starts with deriving the relevant parameters from manufacturer supplied data and some additional tests performed on the motor. These parameters are then translated into set-points and limit values by representing the inverter as a Y-connected voltage source and by investigating the relation between the rated values of the motor and the d/q-components. The implementation steps further include PWM generation with SVPWM and the design of the flux controller and the torque controller with adaptive anti-windup. The input signals are translated into a reference signal for the torque controller. Finally, the power flow management of the series HEV is discussed. For some of the problems encountered during implementation, practical workarounds are presented. *EVS25 Copyright*

Keywords— Field Oriented Control, Hybrid Electric Vehicle, Power Flow Management, SVPWM

1. System description

The HEV that is the subject of this paper consists of an induction motor that is connected (delta connection) to a three-phase inverter. The dc-link of the inverter is fed on the one hand from a battery pack through a bi-directional dc-dc converter and on the other hand from a petrol-engine generator through a power-factor-correction (PFC) converter. The rated values of the motor are as follows: P_N = 4 kW, n_N = 2850 rpm, η_N = 86 %, U_N = 420 V, I_N = 7.8 A, $\cos(\varphi_N)$ = 0.91. The maximum allowable line voltage of the motor in Δ-connection (U_{MAX}) is 242 V. The inverter contains three IGBT half-bridges that produce a pulse-width modulated (PWM) output voltage. The PWM values for the output phases are imposed by the control algorithm that is built using MATLAB/SIMULINK. The inverter has a rated power of 23 kVA and is operated at a switching frequency of 10 kHz. The maximum RMS value of the phase current equals 33 A. The dc-link voltage is chosen to be 400 V_{DC} nominally. The torque produced by the induction motor is controlled using field oriented control (FOC). This control technique is also commonly referred to as vector control.

2. Applied FOC

2.1 Determination of system parameters

A short-circuit test and a no-load test were performed on the induction motor. The results of these tests are presented in table 1.

From these measurements, the values of the elements of the single-phase equivalent circuit (figure 1) can be derived. The resulting parameters are listed in table 2. In figure 1, the symbol V_s is used to indicate the equivalent stator phase voltage.

Table 1: Results of the tests performed on the motor

	Short-circuit test	No-load test
P^* [W]	619/3	245/3
V^* [V]	43/√3	230.7/√3
I^* [A]	14.5	4.27

* phase quantities, f_{AC} = 50 Hz

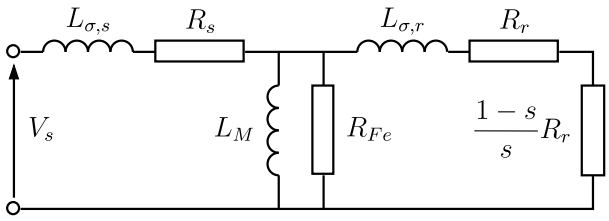

Figure 1: Single-phase equivalent circuit of the induction motor

Table 2: Equivalent circuit parameters

Short-circuit test		No-load test	
$R_{s,r}$	0.5 Ω	R_{FE}	217 Ω
$L_{\sigma s,r}$	2.2 mH	L_M	100 mH

2.2 Transforming phase quantities to quantities in the rotating reference frame

At the foundation of FOC [2] lies the reformulation of the control problem of the induction motor in a rotating reference frame which is synchronised with the instantaneous rotor-flux vector. To this end, the power invariant Clarke transformation (eq. 1) and the Park transformation (eq. 2) are applied to the measured currents [3]. In the rotating reference frame all quantities are decomposed into a set of orthogonal components, i.e. direct ("d") and quadrature ("q") components. The d-axis can be thought of as the flux-generating axis and the q-axis

as the torque-generating axis. The length of the d/q-vectors ($\sqrt{(x_d^2 + x_q^2)}$) can be shown to be $\sqrt{(3/2)}$ times the peak value of the corresponding phase quantity.

The Clark transformation makes the transition from a three-phase system to a two-phase system with two independent axes. The result is a orthogonal reference frame without mutual magnetic coupling, where i_α and i_β are two sinusoidal currents. The Park transformation makes the transition from sinusoidal α/β-variables fixed to the stator to constant d/q-variables fixed to the rotor.

$$\begin{bmatrix} i_\alpha \\ i_\beta \end{bmatrix} = \begin{bmatrix} \sqrt{3/2} & 0 \\ 1/\sqrt{2} & \sqrt{2} \end{bmatrix} \begin{bmatrix} i_a \\ i_b \end{bmatrix} \quad (1)$$

$$\begin{bmatrix} i_d \\ i_q \end{bmatrix} = \begin{bmatrix} \cos\gamma & \sin\gamma \\ -\sin\gamma & \cos\gamma \end{bmatrix} \begin{bmatrix} i_\alpha \\ i_\beta \end{bmatrix} \quad (2)$$

In eq. 2, γ represents the angle between the rotor-flux vector and the stationary α-axis.

Figure 2 shows the phase currents of the induction motor during acceleration. The associated direct and quadrature current components that result from the Park and Clarke transformations are also shown.

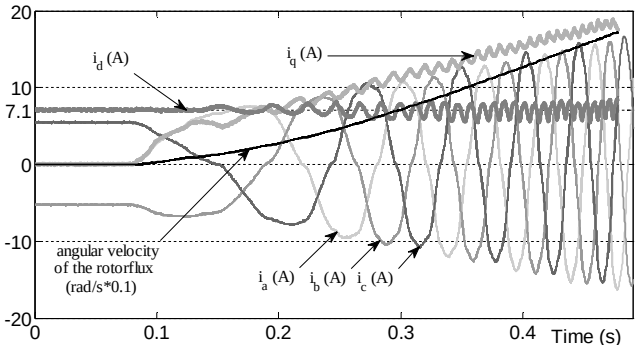

Figure 2: Phase currents, i_q, i_d and ω_μ

2.3 Representation of the induction machine in the d/q-reference frame

According to [2] the electrical behavior of the induction motor is completely described by two stator equations (eq. 3 and 4), two rotor equations (eq. 5 and 6) and a torque equation (eq. 7).

$$\sigma\tau_1 \frac{di_d}{dt} + (1 + \frac{(1-\sigma)\tau_1}{\tau_2}) i_d = \frac{1}{R_s}(u_d - \Delta u_d) \quad (3)$$

$$\sigma\tau_1 \frac{di_q}{dt} + i_q = \frac{1}{R_s}(u_q - \Delta u_q) \quad (4)$$

$$\tau_2 \frac{di_\mu}{dt} + i_\mu = i_d \quad (5)$$

$$\omega_\mu = \omega_r + \omega_{slip} = \omega_r + \frac{i_q}{\tau_2 i_\mu} \quad (6)$$

$$T_{el} = c\Psi_r i_q \quad (7)$$

These equations are expressed in a rotating reference frame, of which the d-axis is aligned with the rotor-flux vector. The parameter *c* in eq. 7 is the torque constant. The quantities u_d and u_q are the d- and q-axis components of the stator voltage, i_d and i_q are the d- and q-axis components of the stator current. The magnetizing current i_μ is defined in eq. 8 and is proportional to the rotor-flux linkage Ψ_r.

$$\Psi_r = \Psi_{rd} = L_M i_\mu \quad (8)$$

Eq. 9 to 11 define the stator time constant τ_1, the rotor time constant τ_2 and the leakage coefficient σ. L_M is the main inductance, $L_s = L_M + L_{\sigma,s}$ is the stator inductance and $L_r = L_M + L_{\sigma,r}$ is the rotor inductance.

$$\tau_1 = \frac{L_s}{R_s} \quad (9)$$

$$\tau_2 = \frac{L_r}{R_s} \quad (10)$$

$$\sigma = 1 - \frac{L_M^2}{L_s L_r} \quad (11)$$

The position of the instantaneous rotor-flux vector, γ, is the algebraic summation of the mechanical rotor angle and the slip angle. The rotor angle is measured by a quadrature encoder. The slip angle is calculated by integrating the slip velocity, which can be calculated by dividing the quadrature current i_q by the product of the magnetizing current i_μ and the time constant of the rotor (eq. 6). The magnetizing current i_μ is obtained as the response of a first order system with i_d as input and a time constant equal to the time constant of the rotor (eq. 5). This is shown in figure 3.

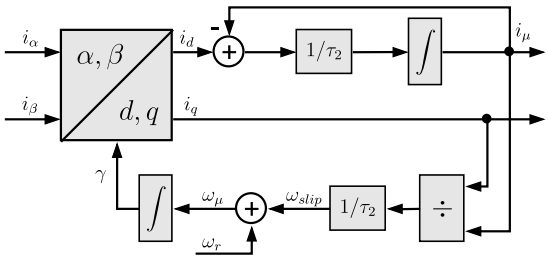

Figure 3: Calculation of the rotor-flux angle

The variables Δu_d and Δu_q, introduced in eq. 3 and 4, represent the non-linear coupling between the stator voltage equations of the d-axis and q-axis. These variables are defined in eq. 12 and 13. When decoupling terms equal to Δu_d and Δu_q are added to the output of the controllers as shown in figure 4, it becomes possible to control the i_d and i_q current components independently from each other. The decoupling terms compensate for the cross-coupling between the d- and q-axis voltages of the induction motor.

$$\Delta u_d = -\sigma L_s \omega_\mu i_q - \frac{L_M^2}{\tau_2 L_r} i_\mu \quad (12)$$

$$\Delta u_q = \sigma L_s \omega_\mu i_d + \omega_r \frac{L_M^2}{L_r} i_\mu \quad (13)$$

Under steady-state operating conditions, the d/q-quantities have a constant value. This makes it possible to attain a very good control performance using a simple PI controller.

The PI controllers, that are used to control the d/q-currents, use anti-windup to prevent the output of the integrator from becoming too large when the set-point cannot be reached within the voltage limits. This improves the dynamic properties of the controller. The limit that has to be imposed on the q-axis voltage depends on the instantaneous d-axis voltage as well as the decoupling terms. Neglecting this dependency would result in a sub-optimal controller since the decoupling terms can grow relatively large towards the higher speed range. This is illustrated in figure 9 where the decoupling terms become dominant at higher speeds. The set-point for the i_q current controller is derived from the input management scheme, whereas the set-point of the i_d-controller is fixed at its nominal value, until field weakening is applied and the direct current becomes inversely proportional to the motor speed.

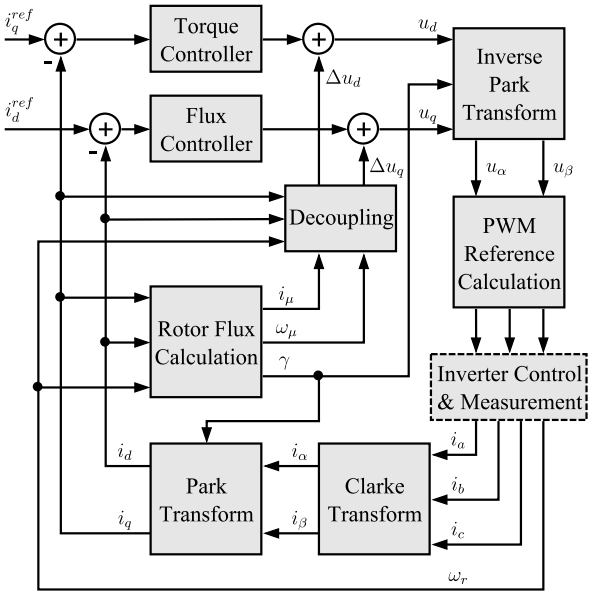

Figure 4: The FOC algorithm

2.4 SVPWM output voltage generation

The desired inverter voltage vector components are calculated by the control algorithm in the rotating reference frame. The inverse Clarke transformation is then applied to these components in order to express the inverter voltages with reference to the stationary α/β-reference frame. The resulting α/β-components are then used to generate the required PWM-values for the inverter phases using an algorithm emulating hardware based space vector modulation (SVM). The α/β-components are scaled with respect to the instantaneous, measured value of the dc-link voltage. This ensures that the output voltage is independent (within limits) of the varying dc-link voltage. Consequently, the output voltage of the inverter can be assumed to be equal to its reference value.

A three-phase two-level inverter can be in one of eight possible switching states. In the α/β-plane, the output voltages associated with these states correspond to six non-zero vectors and two zero vectors. The non-zero state vectors divide the α/β-plane into six sectors. The SVM algorithm determines in which sector the output voltage vector is situated. This procedure is based on simple comparison of the α/β components and does not involve complex calculations.

Within each switching period, the switching patterns associated with the adjacent state vectors are applied successively. The adjacent state vectors are the two non-zero vectors that lie along the edge of the sector that contains the desired output vector, together with the two zero state vectors. The fraction of the switching period each pattern is applied, is determined in such a way that the desired average output voltage is produced.

The control system, that is the subject of this paper, uses space vector pulse-width modulation (SVPWM) [4]. This technique uses the same sector identification procedure as SVM, but instead of actually applying the switching patterns to the switches, this algorithm calculates PWM reference values that produce the same (cycle-average) output voltage. The reference values are then passed on to the pulse-width modulator, which is implemented in the inverter control hardware.

As with conventional SVM, a higher sinusoidal output voltage can be generated for a certain dc-link voltage or, conversely, a lower dc-link voltage is required for a certain output voltage. The phase voltages will contain zero sequence components [5], which are the sum of harmonics with an harmonic order equal to a multiple of three. Those zero-sequence components will not be present in the line voltage that is applied to the motor terminals. This is illustrated in figure 5, where the (cycle-average) phase voltages for both sinusoidal PWM (gray lines) and SVM (black lines) are depicted. Both sets of phase voltages result in the same line voltages (242 V_{rms}), however, the SVM phase voltages can be produced from a lower dc-link voltage. In order for the maximal attainable phase voltage of sinusoidal PWM to be equal to the maximal attainable fundamental component of the SVPWM waveform, the dc-link voltage of the sinusoidal PWM has to be $2/\sqrt{3}$ times higher than the dc-link voltage of SVPWM. In other words, for the same dc-link voltage, the rms value of the fundamental component of the SVPWM phase voltage is $2/\sqrt{3}$ times the rms value of the sinusoidal PWM phase voltage.

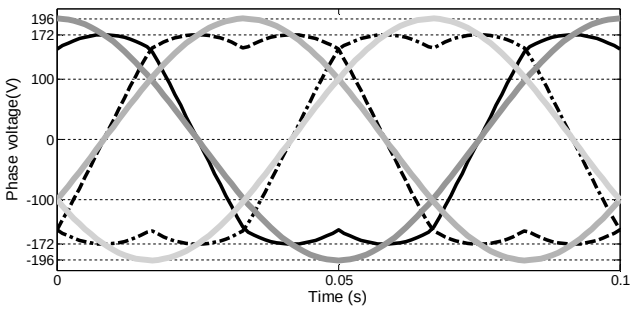

Figure 5: Inverter phase voltages for SV(PW)M and sinusoidal PWM.

2.5 Calculation of the nominal and limit values for $u_{q/d}$ and $i_{q/d}$

A three-phase inverter (figure 6) can be represented as a three-phase Y-connected voltage source. In this representation each half bridge of the inverter is replaced by a voltage source, situated between the output of the half bridge and the middle of the dc-link (figure 7). As shown in figure 6, the voltage of the equivalent voltage source U_{a0} can be measured between the output a of the first half bridge and *'0'*, the middle of the dc-link. The measured voltage U_{a0} has a maximal value of $U_{dc}/2$ when the top switch of the half bridge is closed and a minimal value of $-U_{dc}/2$ when the bottom switch of the half bridge is closed. The amplitude of a sinusoidal waveform is $\sqrt{2}$ times the rms-value of the waveform. Assuming that the inverter is producing an undistorted, purely sinusoidal voltage, the maximal attainable rms-value of the produced phase voltage U_{a0} is $(U_{DC}/2)/\sqrt{2}$ for sinusoidal PWM. As explained in 2.4, the rms-value of the fundamental component of the SVPWM phase voltage is $2/\sqrt{3}$ times higher than the rms-value of the sinusoidal PWM phase voltage, resulting in an rms-value for the fundamental component of $U_{DC}/\sqrt{6}$. The rms-value of the line voltage U_{ab} is $\sqrt{3}$ times the rms-value of the phase voltage when using sinusoidal PWM, resulting in a maximal rms-value of the inverter line voltage of $\sqrt{3/2}(U_{DC}/2)$. However, in this work SVPWM is used, enabling the rms-value of the inverter line voltage to reach $U_{DC}/\sqrt{2}$. The phase voltage of the motor in Δ-connection is equal to the line voltage U_{ab} of the inverter in this set-up. As the nominal phase voltage of the motor is 242 V, this results in a minimal dc-link voltage of approximately 345 V. The nominal dc-link voltage is 400 V, allowing the dc-link voltage to drop during low-load to high-load transitions without compromising the functioning of the induction motor.

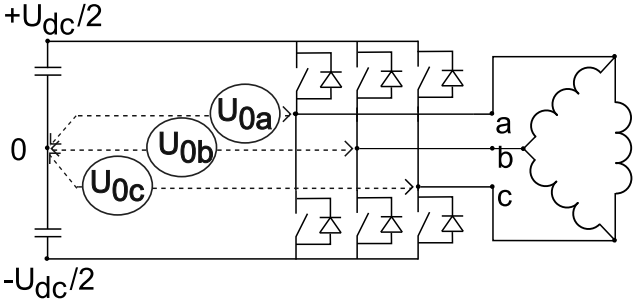

Figure 6: Three-phase inverter with Δ-connected motor and measurement of the equivalent phase voltages of each half bridge

In order to calculate the nominal values of the direct and quadrature voltages and currents, the relation between these values and the nominal values of the induction motor must be known. A first step is the relation between the rms-values of the current and voltage in the α/β-reference frame and the (a,b,c)-reference frame. These relations are given in eq. 14 and 15 [2] for the power invariant Clarke transformation described in eq. 1.

$$I_{\alpha,rms} = I_{\beta,rms} = \sqrt{\frac{3}{2}} I_{a,rms} \tag{14}$$

$$U_{\alpha,rms} = U_{\beta,rms} = \sqrt{\frac{3}{2}} U_{a,rms} \tag{15}$$

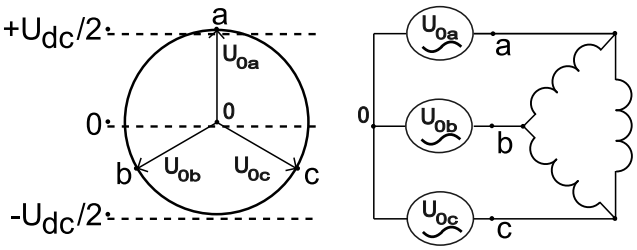

Figure 7: Equivalent representation of the inverter as a Y-connected three-phase voltage source coupled to a Δ-connected motor

The stator-fixed α/β-reference frame is transformed to the rotor-fixed rotating d/q-reference frame by the Park-transformation described in (2). The length of the dq-vectors, $\sqrt{(x_d^2 + x_q^2)}$, which are time-invariant in steady state, are equal to the length of the αβ-vectors, $\sqrt{(x_\alpha^2 + x_\beta^2)}$. The length of these vectors is equal to the amplitude of the α/β-waveforms. Assuming sinusoidal currents and voltages, the relation between the amplitude and rms-value of the α/β-waveforms is $\sqrt{2}$, resulting in eq. 16 and 17.

$$\sqrt{i_d^2 + i_q^2} = \sqrt{2} I_{\alpha,rms} = \sqrt{2} I_{\beta,rms} = \sqrt{3} I_{a,rms} \tag{16}$$

$$\sqrt{u_d^2 + u_q^2} = \sqrt{2} U_{\alpha,rms} = \sqrt{2} U_{\beta,rms} = \sqrt{3} U_{a,rms} \tag{17}$$

In order to deduce practical values for u_d, i_d, u_q and i_q, it must be noted that the (a,b,c)-voltages and currents described in eq. 14 to 17 represent the rms-values of the fundamental component of the phase voltage and current of the Y-connected inverter equivalent of figure 7.

As mentioned, the phase voltage of the motor equals the line voltage of the inverter and has a nominal value of 242 V. As the line voltage of a Y-connection is $\sqrt{3}$ times the phase voltage, the nominal value of $u_{d,q}$, $U_{d,q,nom}$, is derived from the nominal phase voltage of the motor in eq. (19).

$$U_{d,q,nom} = \sqrt{U_{d,nom}^2 + U_{q,nom}^2} \tag{18}$$

$$U_{d,q,nom} = \sqrt{3} U_{inverter,phase,rms} = \sqrt{3} \frac{U_{inverter,line,rms}}{\sqrt{3}} = 242 \text{ V} \tag{19}$$

Thus, $U_{d,q,nom}$, as defined in eq. 18, is equal to the nominal inverter line voltage. The nominal value of u_q, $U_{q,nom}$, was chosen to be 230 V. This value must be as high as possible, without exceeding the insulation voltage limits, as this voltage is responsible for keeping the quadrature current at its set-point in spite of the large back-emf. Taking into account the values of $U_{d,q,nom}$ and $U_{q,nom}$, this allows a nominal value of u_d, $U_{d,nom}$, of 75 V. Tests (figure 10 a.o.) revealed that u_d varies approximately between -55 and 55 V, so the i_d-controller will not have any problems maintaining i_d at the requested set-point.

The nominal phase current of the induction motor is 7.8 A. As the motor is Δ-connected, the resulting line current is $\sqrt{3}$ times the phase current or 13.5 A. This line current equals the phase current of the Y-connected inverter. According to (16), this results in a nominal $i_{d,q}$, $I_{d,q,nom}$, which is $\sqrt{3}$ times the rms-value of the phase current of the inverter or 23.4 A. Thus, $I_{d,q,nom}$ is equal to 3 times the nominal phase current of the Δ-connected motor.
As the nominal current of the motor is 7.8 A and $\cos(\varphi_N)$ equals 0.91, this results in a reactive current of 3.23 A. Assuming all of the reactive current is used to produce the rotor flux, this would result in a nominal i_d current, $I_{d,nom}$, of 9.7 A. However, an actual test proved to be more reliable than a calculation based on the nominal values. The test involves the motor being driven by the inverter with an open loop voltage/frequency control at the nominal frequency, while the current measurements are being transformed to d,q values. This test revealed a direct current of 7.1 A, which was set as the nominal value. This nominal value is maintained until 2700 rpm, after which field weakening is applied and i_d declines inversely proportional with the measured rotor speed. The 2700 rpm value is below the nominal speed of 2850 rpm. This is necessary to allow the motor to go beyond the nominal speed. If the field weakening is postponed to 2850 rpm, the back-emf, which is represented by the decoupling term Δu_q (13) [6], will become too large. As both i_d/i_μ and ω_μ/ω_r simultaneously reach high values at the nominal speed, the back-emf becomes higher than the nominal u_q value of 230 V. This situation can be avoided by applying the field weakening at a lower speed, such that i_d/i_μ is already declining at nominal speed. As can be seen in figure 9, the inverter is now able to produce a sufficiently large u_q to allow i_q to reach its nominal value.
As $I_{d,q,nom}$ is the algebraic sum of $I_{d,nom}$ and $I_{q,nom}$ and $I_{d,q,nom}$ and $I_{d,nom}$ are 23.4 A and 7.1 A respectively, $I_{q,nom}$ is set at 22.3 A. At low speeds, the maximal i_q value, $I_{q,max}$, is raised to 35 A, resulting in a maximal $I_{d,q}$ of 35.7 A and a maximal inverter output current of 20.6 A. This value is well below the nominal inverter current of 33 A, so the inverter can easily provide the augmented currents. By increasing the torque at lower speeds a more powerful acceleration is achieved. As the currents at this low speeds will be higher than the nominal currents, an independent fan cools the induction motor to prevent excessive heating.

2.6 PI torque-controller with adaptive anti-windup

As discussed in section 2.3, decoupling terms equal to Δu_d and Δu_q (eq. 12 and 13) must be added to the direct and quadrature voltages u_d and u_q to enable independent control of both d/q-currents. In figure 8 this is achieved by adding the decoupling term $u_{q,decoupling}$ to the output of the controller, $u_{q,reg}$. The resulting u_q is converted to the appropriate reference signal for the inverter control hardware by the inverse park transformation and the SVPWM algorithm.

$U_{q,decoupling}$ can reach values as high as the maximal allowable quadrature voltage, which is confined between $+U_{q,lim}$ and $-U_{q,lim}$. When using a PI controller with anti-windup limits for the integrating part, $u_{q,int}$, fixed at $+U_{q,lim}$ and $-U_{q,lim}$, the decoupling term $u_{q,decoupling}$ creates an offset, around which the controller operates. The resulting u_q is thus restricted to values between $u_{q,decoupling}+U_{q,lim}$ and $u_{q,decoupling}-U_{q,lim}$ when neglecting the proportional part $u_{q,prop}$ of the controller. For example, assume $u_{q,decoupling}$ is equal to $+U_{q,lim}$ at high positive speeds, the controller can regulate u_q between $2U_{q,lim}$ and 0, which is reduced between $U_{q,lim}$ and 0 after the final saturator. A positive current error could now force $u_{q,int}$ to grow as large as $U_{q,lim}$. When a negative current error occurs at the input of the controller, the output of the final saturator will only start to decline after $u_{q,int}$ has dropped from $U_{q,lim}$ to 0. This behaviour is not what we expect from a controller with anti-windup.

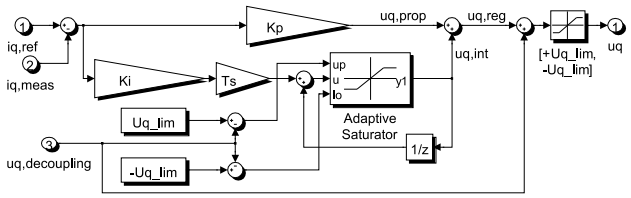

Figure 8: PI controller with adaptive anti-windup

The situation can be improved by implementing a PI controller with adaptive anti-windup limits, depicted as *Adaptive Saturator* in figure 8. By subtracting $u_{q,decoupling}$ from the fixed limits $U_{q,lim}$ and $-U_{q,lim}$, adaptive limits are obtained which allow $u_{q,int}$ to vary between $U_{q,lim}-u_{q,decoupling}$ *and* $-U_{q,lim}-u_{q,decoupling}$. This allows the PI controller to regulate u_q between $+U_{q,lim}$ and $-U_{q,lim}$, irrespective of the value of $u_{q,decoupling}$. The integrator is disabled when the output of the controller tends to exceed its limits. Clearly, using a saturator with fixed limits undermines the anti-windup function of the saturator and renders it useless.

The behaviour of the PI controller and the resulting i_q is demonstrated in figure 9. This figure illustrates the acceleration of the motor from standstill to maximal speed in 1 s. The tires are allowed to spin freely. Clearly the decoupling term is very large at higher speeds. Nonetheless, the nominal value of i_q can be achieved.

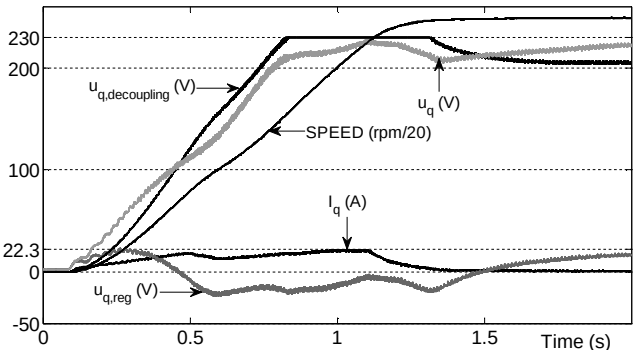

Figure 9: Quadrature voltages and resulting iq during acceleration

2.7 PI flux-controller

The direct current i_d is controlled by regulating the direct voltage u_d. As mentioned in 2.5, the set-point of i_d is 7.1 A up to 2700 rpm. Above this speed field weakening is

applied and the set-point declines inversely proportional with the measured rotor speed. The i_d-controller is a simple PI controller with anti-windup which does not take the decoupling term Δu_d into account. The anti-windup limits the integrating part of the controller between -75 and +75 V. The output of the controller $u_{d,reg}$ is augmented by the decoupling term $u_{d,decoupling}$. The resulting sum u_d is again saturated between -75 and +75 V. Figure 10 shows the behaviour of the controller and decoupling term during acceleration from standstill to maximal speed. Both the controller output $u_{d,reg}$ and the total u_d stay within the 75 V limit. Clearly, the controller is able to regulate i_d without taking the decoupling term into account.

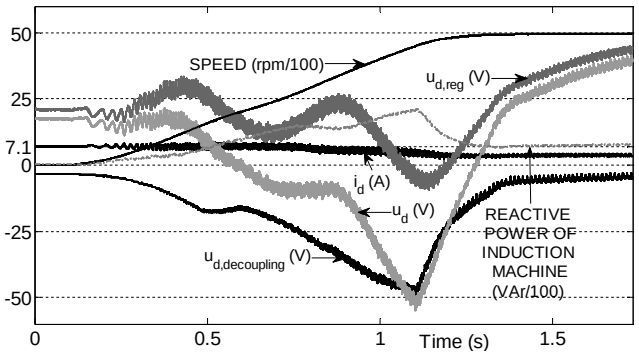

Figure 10: Direct voltages and resulting i_d during acceleration

3. Input Management Scheme

The driver can communicate with the control scheme by means of three inputs; the accelerator, the brake pedal and a switch to choose between the forward and backward driving direction. The input management scheme is part of the motor control scheme and uses the three inputs to calculate the appropriate value of the torque producing current i_q. The accelerator is linked to a 1kΩ linear potentiometer via a cable. The resistance of this potentiometer can vary between 20 Ω, when the accelerator is at rest, and 960 Ω, when the accelerator is fully pressed down. This signal is linearly translated into a signal between 0 and 1. The brake pedal is also linked to a 1kΩ linear potentiometer, which varies between 106 and 860 Ω and which is also linearly translated in a 0 to 1 signal. The distinction with the accelerator is that this pedal is also linked to a mechanical disc brake through a cable. The first part of the stroke of this pedal only actuates the potentiometer, allowing purely regenerative braking. In the second part of the stroke regenerative braking is combined with disc braking. At the end of the first part of the stroke, before the mechanical brake is actuated, the regenerative braking power is at its maximum. The forward/backward switch has only two states, 0 and 1000 Ω, which is translated in a -1 and +1 signal respectively. This signal is routed to a subroutine that passes on the previous state of the signal when the absolute speed is above 50 rpm and the current state of the signal when the speed is below 50 rpm. The accelerator and brake signal are only passed on when the signal is above 0.1 to avoid activation of the vehicle when the driver's foot is merely resting on the pedal.

3.1 Accelerator pedal

The nominal value of i_q, $I_{q,nom}$, is 22.3 A, while the maximal value of i_q, $I_{q,max}$, is set at 35 A. The accelerator signal, acc_{in}, is multiplied by a speed dependent maximal value of i_q, $i_{q,max}(n)$, to obtain the absolute value of the set-point for the I_q-controller. In the following, the calculation of $i_{q,max}(n)$ is explained. The scheme that implements this calculation is depicted in figure 11. As long as the motor speed is below 1500 rpm, $i_{q,max}(n)$ is set at the maximal value of 35 A. Between 1500 and 2000 rpm, $i_{q,max}(n)$ is lowered from $I_{q,max}$ to $I_{q,nom}$. The value of $i_{q,max}(n)$ in this interval is calculated based on eq. 20.

$$i_{q1}(n) = I_{q,\max} + \frac{I_{q,nom} - I_{q,\max}}{N_{iq,nom} - N_{iq,\max}}(|n_{meas}| - N_{iq,\max}) \qquad (20)$$

In this equation, $I_{q,max}$ is 35 A, $I_{q,nom}$ is 22.3 A, $N_{iq,max}$ is 1500 rpm, $N_{iq,nom}$ is 2000 rpm and n_{meas} is the measured speed. The first switch in figure 11 passes on $I_{q,max}$ when the speed is below $N_{iq,max}$ and $i_{q1}(n)$ when the speed is higher. This allows an increase of the available torque from 13.4 Nm to 21 Nm below 1500 rpm, but it also means that the motor delivers 3.3 kW mechanical power at 1500 rpm. This range can be extended to 1800 rpm at which point the motor delivers 4 kW mechanical power and consumes 4.65 kW electrical power. Any increase of the maximum torque range beyond 1800 rpm will result in the motor consuming more power than the battery can deliver, which is not allowed. To maintain a certain margin, the maximum torque range was limited to 1500 rpm. The second switch passes on the value of the first switch when the speed is below $N_{iq,nom}$ and $I_{q,nom}$ when the speed is higher. The third switch passes on the value of the second switch when the speed is below $N_{run\text{-}down}$ and $i_{q2}(n)$ when the speed is higher. The current $i_{q2}(n)$ is based on eq. 21.

$$i_{q2}(n) = I_{q,nom}(1 - \frac{|n_{meas}| - N_{run-down}}{N_{\max} - N_{run-down}}) \qquad (21)$$

In this equation, N_{max} equals 5000 rpm and $N_{run\text{-}down}$ equals 4500 rpm.

The fourth switch passes on the value of the third switch when the speed is below N_{max} and 0 when the speed is higher. This allows a smooth transition from full torque at $N_{run\text{-}down}$ to zero torque at N_{max}. If the quadrature current switches from $I_{q,nom}$ to 0 at N_{max}, the motor starts to oscillate at this speed, because the applied torque drives the vehicle beyond N_{max}, at which point the torque drops to zero, causing the vehicle to slow down below N_{max}, where the cycle will start again. This maximum $i_{q,max}(n)$ value is valid as long as the battery is not considered discharged.

When the battery management alerts the upper level control scheme of a discharged battery, the input signal "empty batt" forces the sixth switch to pass on the output of the fifth switch. The motor power is now limited to P_pfc_lim, which is equal to 700 W. This allows the petrol-engine generator to simultaneously charge the battery and provide the motor with power. This will of course result in a strongly reduced speed. The output of the fifth switch is a reduced i_q value, $i_{q,red}(n)$, When this

value is used as a reference for i_q, the the power consumed by the induction motor is limited to P_pfc_lim. At low speeds $i_{q,red}(n)$ is higher than $i_{q,max}(n)$, so the fifth switch will relay $i_{q,max}(n)$ when this is the case. The way in which $i_{q,red}(n)$ is calculated, is explained in the brake pedal paragraph. The result of this scheme is depicted in figure 14. The obtained $i_{q,out,acc}$ is the result of the state of the accelerator, acc_{in}, multiplied by the speed dependent $i_{q,max}(n)$ or $i_{q,red}(n)$ value. As mentioned, acc_{in} is 0 when the accelerator is at rest and linearly increases to 1 when the accelerator is fully pressed down. The obtained $i_{q,out,acc}$ is in turn multiplied by the sign derived from the forward/backward switch and thus becomes the set-point for the quadrature current when the accelerator is engaged.

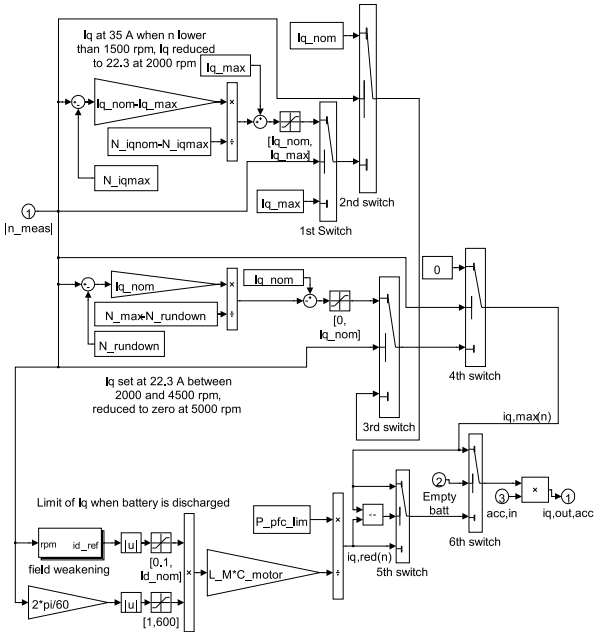

Figure 11: Calculation of maximal i_q during acceleration

3.2 Brake pedal

As explained, the state of the brake pedal is transformed into a signal between 0 and 1, taking into account that values below 0.1 are not passed on. In a next step, the signal is set to zero when the absolute value of the speed is below 50 rpm. When the speed is higher than 50 rpm the signal is passed on unaffected. This allows the motor to switch off I_q at standstill and avoids problems with oscillating brake torques when the speed is near zero. Next, the sign of the brake torque is determined. When the vehicle is moving forward respectively backward, the speed is positive respectively negative and the torque needs be negative respectively positive to slow the vehicle down. It is important to note that the sign of the brake torque should not depend upon the state of the forward/backward switch, since this may cause a vehicle that is put in forward but accidently goes backward, e.g. when starting on a slope, to unintentionally start to accelerate backwards when the brake is applied. The signal is now multiplied by the obtained sign, resulting in $brake_{in}$ (figure 12). The signal $brake_{in}$ is multiplied by the speed dependent maximal i_q value during braking, $i_{q,brake}(n)$. This value is based on eq. 7, which gives the electromagnetic torque, T_{el}, in terms of the torque constant, *c*, and the rotor flux linkage, Ψ_r. The rotor flux linkage is calculated with eq. 8.

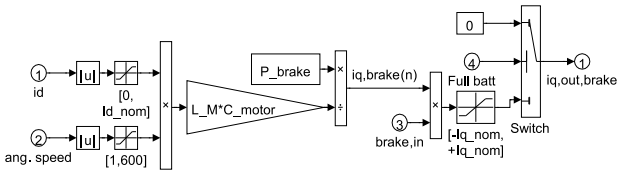

Figure 12: Calculation of maximum i_q during braking

The relation between the magnetizing current i_μ and direct current i_d is given by eq. 5. From this relation it follows that, in steady state, the magnetizing current i_μ and direct current i_d are equal. In order to simplify the calculations, Ψ_r is approximated according to eq. 22.

$$\Psi_r \cong L_M i_d \tag{22}$$

The main inductance L_M of 100 mH was determined by the no-load test and i_d is measured. The only unknown parameter in eq. 7 is the torque constant *c*, which is approximated by C_M. C_M is determined by matching the nominal torque to the nominal i_q current. By substituting eq. 22 in eq. 7 and by taking into account that the nominal torque is calculated by dividing the nominal mechanical power by the nominal radial frequency, eq. 23 is obtained.

$$T_{el,nom} \cong P_{nom}/\omega_{nom} = C_M L_M I_{d,nom} I_{q,nom} \tag{23}$$

In this equation the electric torque is assumed to be equal to the mechanical torque. Although this assumption neglects the friction losses etc., it provides a practical workaround to calculate an approximate value C_M for *c*.
By substituting the variables from eq. 23 by the real values, eq. 24 is obtained.

$$\frac{4000W}{(2850\ rpm * 2\pi/60)} = C_M * 100mH * 7.1A * 22.3A \tag{24}$$

Eq. 24 results in C_M = 0.847. Now the motor constant is known and the maximum value $i_{q,brake}(n)$ during deceleration can be calculated with eq. 25.

$$i_{q,brake}(n) = P_{brake} / C_M L_M i_d \omega_r \tag{25}$$

In eq. 25, C_M and L_M are known parameters and i_d and ω_r are calculated based on measurements. The implementation of this equation is depicted in figure 12. P_{brake} is set at 750 W, which results in a maximal charging current of approximately 10 A when the battery voltage is 75 V. This is more than the recommended charging current, but AGM batteries are able to cope with charge abuse due to their water based electrolyte and charging currents up to 0.4 times the capacity are allowed, certainly when this occurs in short bursts, as is common for regenerative braking. Given a capacity of 30 Ah, this results in a upper limit of 12 A for the charging current. The obtained $i_{q,brake}(n)$ is multiplied by the signed state of the brake pedal, $brake_{in}$. As $i_{q,brake}(n)$ is inversely proportional with the speed, it becomes extremely high at low speeds. In order to limit the torque during regenerative

braking, a saturator limits the result of $i_{q,brake}(n)*brake_{in}$ between $-I_{q,nom}$ and $+I_{q,nom}$. To protect the battery when it is fully charged, regenerative braking is disabled by the upper level control scheme. In that case the input signal "full batt" forces the output of the switch, $i_{q,out,brake}$, to zero when the brake pedal is applied. In all other circumstances $i_{q,out,brake}$ equals the saturated value of $i_{q,brake}(n)*brake_{in}$.

In figure 13, the motor voltages and currents are depicted during deceleration. It is clear from this figure that the controller attempts to maintain the braking power at 750 W. To this end, i_q is adjusted according to eq. 25.

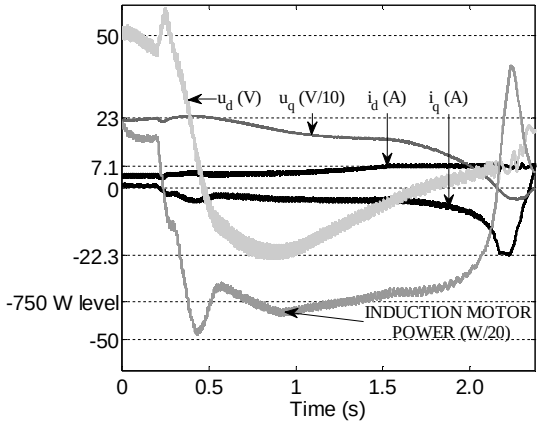

Figure 13: Quadrature and direct voltages and currents and induction motor power during regenerative braking

3.3 Determination of i_q set-point

Both the accelerator and the brake pedal are able to control the set-point of i_q. In order to secure a safe operation of the vehicle, the brake pedal will have priority over the accelerator when both are actuated at the same time. The last part of the input management scheme is a rate limiter that limits the change of the torque producing quadrature current i_q to 210 A/s. This is beneficial for the stability of the dc-dc converter that controls the dc-link voltage. The maximum values of i_q during acceleration and braking are depicted in figure 14. When neglecting the reduction of i_q near the maximal rpm, the maximal values of i_q in all cases become constant above 2700 rpm, the speed at which field weakening is applied. Here, the reduction in i_d will limit the power of the motor.

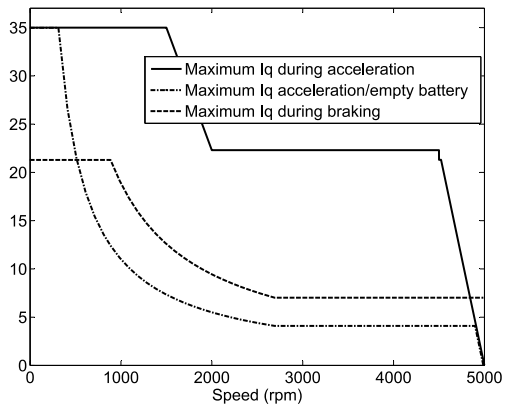

Figure 14: Maximum value of Iq in function of motor speed.

4. Supervisory control scheme

The supervisory control is the power flow management part of the control scheme (figure 15). Hierarchically, it is situated above the control schemes of the motor, PFC boost converter and dc-dc converter. The supervisory control's main functions are the optimal use of the petrol-engine generator and the protection of the battery against overcharging and over-discharging.

4.1 Battery management

A look-up table (LUT), based on data provided by the battery manufacturer, together with voltage and current measurements, is used to determine whether the battery is empty, full or in-between. When the battery voltage drops below a certain current-dependent voltage threshold, the battery is considered empty. As soon as the *empty* state is detected, an integrator is activated that uses the battery voltage and current to monitor the energy delivered to the battery. Using the value of the current multiplied by minus one, results in an increase of the integrator value, which represents the energy delivered to the battery, when the current is flowing from the dc-link to the battery and vice-versa. The integrator maintains the battery state at *empty* as long as the total energy delivered to the battery is below 100 Wh. As long as the battery state is set to *empty*, the motor power is limited to 700 W by lowering the allowable current i_q as discussed in section 2.7. When the integrator reaches 100 Wh, the battery is no longer considered empty and full motor power is restored.

Similarly, the battery will be considered full when the battery voltage reaches a fixed threshold of 104 V. A second integrator will keep the battery at the *full* state as long as the battery has been discharged with less than 100 Wh. As long as the battery state is set to *full*, regenerative braking is disabled by keeping i_q at zero during braking.

The hysteresis provided by the integrators, prevents erratic switching between operating regions.

4.2 Generator management

Due to the poor efficiency of the portable generator at partial loading, the decision was made to operate the portable generator at 1.2 kW. As the efficiency of the PFC boost converter, which connects the generator with the dc-link, is 90 % at an input power of 1.2 kW, the measured output power at that instant is 1.08 kW. The supervisory control scheme uses this value as set-point for the generator when its operation is deemed advantageous. Otherwise the set-point for the generator is set to zero. The set-point of the generator will be adapted based on the measured power consumption P_{IM} of the induction machine, which is obtained by applying eq. 26.

$$P_{IM} = u_d i_d + u_q i_q \tag{26}$$

When the battery state is set to *full*, the generator set-point is 0 as long as P_{IM} is below 1080 W. All power is delivered by the battery. As soon as P_{IM} is above 1080 W, the generator provides 1.08 kW. The remaining power is delivered by the battery. The generator will only provide traction power in this mode and will not charge the

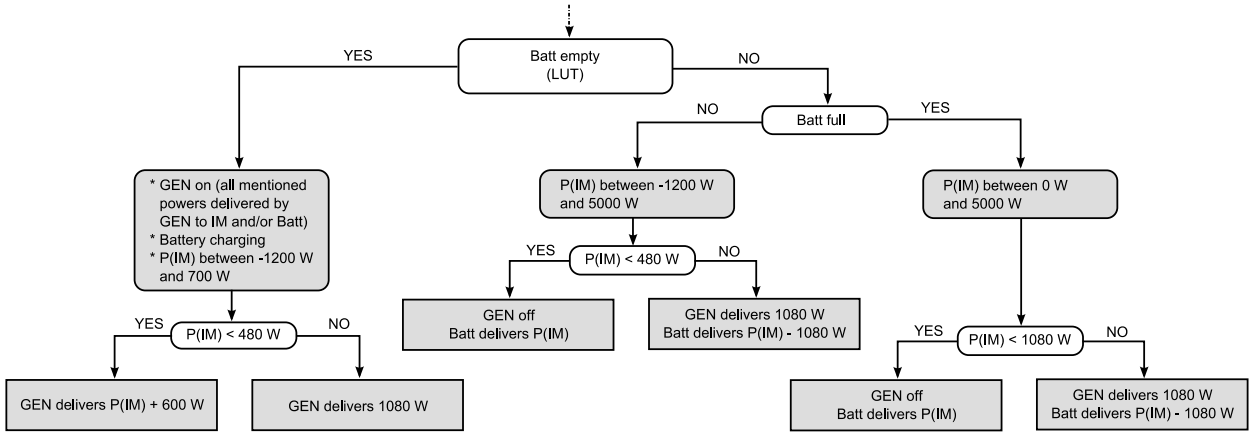

Figure 15: Supervisory control scheme for energy flow management

batteries.

When the battery state is between *full* and *empty*, the generator set-point is set to zero as long as P_{IM} is below 480 W. All power is delivered by the battery. As soon as P_{IM} is above 480 W, the generator provides 1.08 kW. This will result in the charging of the battery when P_{IM} is between 480 and 1080 W. The charging power is 600 W when P_{IM} is 480 W and linearly decreases to zero when P_{IM} reaches 1080 W. Above 1080 W, traction power is shared between the generator and battery, where the generator will deliver 1.08 kW and the remainder is provided by the battery.

The fixed set-point for the generator power is abandoned when the battery state is *empty* and the generator becomes the only source of power. When the induction machine generates between -1200 and – 600 W during regenerative braking, the set-point of the generator is set to zero, otherwise the combined power of the induction machine and generator would overcharge the battery. The set-point of the generator increases linearly from zero when P_{IM} equals -600 W to 1080 W when P_{IM} equals 480 W, resulting in a constant charging power of 600 W in this interval. A further increase of the motor power beyond 480 W is prevented by the input management scheme.

4.3 Collaboration between supervisory control scheme and lower level control schemes.

Firstly, the supervisory control scheme manages to protect the battery against overcharging and over-discharging by monitoring the battery current and voltage. The supervisory control scheme can limit the motor power, both during driving as during regenerative braking, by sending the appropriate signals to the input management scheme. The input management scheme interprets these signals and independently calculates the maximal allowable quadrature current i_q, both during acceleration and deceleration, based on the motor speed. The supervisory control scheme will consider the battery as empty or full, until the battery has been charged or discharged sufficiently, respectively. This allows the battery to recover before full discharge or charge power is applied and prevents erratic switching between different modes of the battery state.

Secondly, the motor control scheme provides the supervisory control scheme with the power consumed by the motor. The supervisory control scheme provides the PFC control scheme with a set-point of 1.08 kW, allowing the generator to operate at its optimal working point of 1.2 kW, while simultaneously charging the battery when traction power is low. However, when the battery is empty and the generator becomes the only source of power, priority is given to the mobility of the vehicle and charging of the battery. In this case the set-point provided to the PFC control scheme varies between zero and full power, despite the loss of efficiency at a partial load.

Figure 16 shows the power provided by the battery and petrol-engine generator during acceleration of the vehicle while the battery state is between *full* and *empty*. As soon as the motor power exceeds 480 W, the petrol-engine generator is turned on and delivers the expected 1.08 kW. As the accelerator pedal is released, the motor power drops below the 1.08 kW level and the petrol-engine generator recharges the battery.

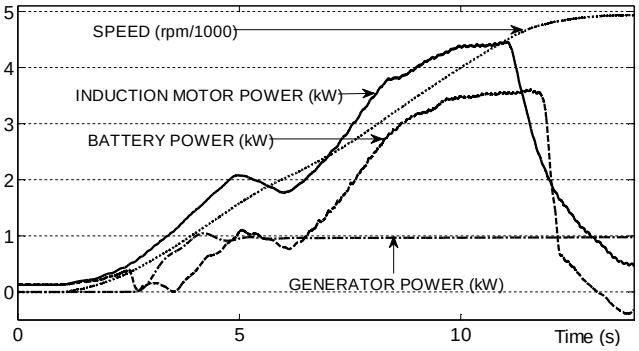

Figure 16: Power of induction motor, battery and generator during acceleration

5. Conclusion

A first step in applying FOC is the measurement of the equivalent circuit parameters. In a next step the Clarke and Park transformations can be introduced along with the rotor flux calculation and decoupling terms. Up to this point it is possible to drive the motor by the inverter with an open loop voltage/frequency control scheme. This allows to compare the obtained values of the quadrature and direct voltages and currents with the expected values. The expected values can be calculated by representing the inverter as a three phase Y-connected voltage source which supplies the induction motor and by taking the relation between the (a,b,c)-reference frame and the d/q-reference frame into account.

Once the representation of the currents and voltages in the d/q reference frame is successfully implemented, it becomes possible to control the induction machine. On the one hand the produced flux can be controlled by implementing a simple anti-windup PI-controller which controls i_d by adjusting u_d. On the other hand the produced torque can be controlled by implementing an anti-windup PI-controller with an adjustable saturator which controls i_q by adjusting u_q. Here the back-emf, which is represented by the decoupling term Δu_q, is incorporated into the anti-windup limits of the integrating part of the controller, allowing the design of a robust controller.

The d/q-voltages at the output of the controllers are transformed into α/β-voltages by the inverse Clarke transformation. The α/β-voltages are used to generate PWM-values for the inverter phases with a SVPWM algorithm. This algorithm allows to produce the required voltages with the minimal dc-link voltage.

The set-point for the torque controller is generated by the input management scheme. This scheme translates the state of the accelerator and brake pedal, together with the forward/backward switch into a speed dependent set-point taking the necessary safety measures into account.

The supervisory control scheme manages the power delivered by the battery and petrol-engine generator in such a way that the petrol-engine generator operates at maximal efficiency. When the battery is considered full or empty, the motor power will be adapted such that the battery cannot be damaged by overcharging during regenerative braking or over-discharged during driving. This scheme allows the motor, battery and petrol-engine generator to operate in a coordinated fashion.

6. References

[1] P. Tant et al., “Case-study of an Educational Engineering Project: a Series Hybrid Electric Kart", Journal sur l'enseignement des sciences et technologies de l'information et des systèmes, Vol. 8, 2009

[2] Terörde G., “Electrical Drives and Control Techniques”, Published by Uitgeverij Acco (ISBN 90-334-5686-9), Leuven, 2004, 378 pages.

[3] Bose B.K., “Power Electronics and Variable Frequency Drives: Technology and Applications”, Edited by Bimal K. Bose, IEEE Press, New York, 1997.

[4] Wei-Feng Zhang, Yue-Hui Yu, “Comparison of Three SVPWM Strategies”, Journal of Electronic Science and Technology of China, Vol. 5, no. 3, September 2007, pp. 283-287

[5] Keliang Zhou, Danwei Wang, “Relationship Between Space-Vector Modulation and Three-Phase Carrier-Based PWM: A Comprehensive Analysis”, IEEE Transactions on Industrial Electronics, Vol. 49, no. 1, February 2002, pp. 186-196.

[6] Sheng-Ming Yang, Chen-Haur Lee, “A Deadbeat Current Controller for Field Oriented Induction Motor Drives”, IEEE Transactions on Power Electronics, Vol. 17, no. 5, September 2002, pp. 772-778.

7. Authors

Ir. Kristof Engelen
Esat-Electa, KULeuven, Kasteelpark Arenberg 10, 3001 Heverlee, Belgium
Tel: +32 16 32.10.26
Fax: + 32 16 32.19.85

Kristof Engelen received the M.Sc. degree in electrical engineering from Katholieke Universiteit Leuven (K.U. Leuven), Leuven, Belgium, in 2005. He is currently a Research Assistant at K.U. Leuven ESAT/ELECTA, where he is working toward the Ph.D. degree. His research interests include power electronics and its applications.

Ir. Sven De Breucker
ETE, Vito, Boeretang 200, 2400 Mol, Belgium
Tel: +32 14 33.58.27
Fax: +32 14 32.11.85

Sven De Breucker was born in 1980 in Belgium. He received the M.Eng. degree in Electromechanics in 2002 from the De Nayer University College and the M.Sc. degree in Electrotechnical Engineering in 2007 from the KULeuven (Catholic University of Leuven), Belgium and is currently pursuing a Ph. D. in Electrotechnical Engineering at the Research Group ELECTA, KULeuven. His main interests are power electronics and hybrid electric vehicles. His research focuses on dc-dc converters and batteries.

.

Prof. dr. ir. Johan Driesen
Esat-Electa, KULeuven, Kasteelpark Arenberg 10, 3001 Heverlee, Belgium
Tel: +32 16 32.10.24
Fax: + 32 16 32.19.85
Email: Johan.Driesen@esat.kuleuven.be

Johan Driesen (S’93–M’97) was born in 1973 in Belgium. He received the M.Sc. degree in 1996 as Electrotechnical Engineer from the K.U.Leuven, Belgium. He received the Ph.D. degree in Electrical Engineering at K.U.Leuven in 2000 on the finite element solution of coupled thermal-electromagnetic problems and related applications in electrical machines and drives, microsystems and power quality issues. Currently he is a professor at the K.U.Leuven and teaches power electronics and drives. In 2000-2001 he was a visiting researcher in the Imperial College of Science, Technology and Medicine, London, UK. In 2002 he was working at the University of California, Berkeley, USA. Currently he conducts research on distributed generation, including renewable energy systems, power electronics and its applications, for instance in drives and power quality.